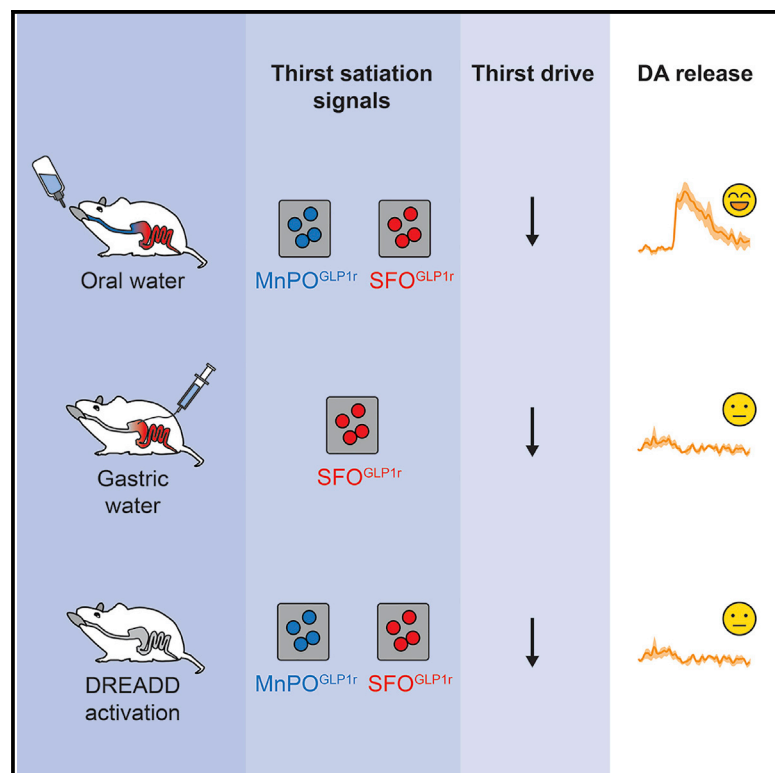


Temporally and Spatially Distinct Thirst Satiation Signals

Graphical Abstract



Authors

Vineet Augustine, Haruka Ebisu, Yuan Zhao, ..., Grace O. Mizuno, Lin Tian, Yuki Oka

Correspondence

yoka@caltech.edu

In Brief

The mammalian thirst circuit receives temporally distinct satiation signals by both liquid gulping action and gut osmolality sensing. These thirst satiation signals are functionally separable from the reward-related circuit activity.

Highlights

- Thirst neurons in the brain receive temporally distinct multiple satiation signals
- Liquid gulping and gut osmolality signals transmit thirst satiation
- Specific GABAergic neurons in the subfornical organ (SFO) mediate satiation signals from the gut
- Drinking-induced dopamine release is independent of thirst satiation signals



Temporally and Spatially Distinct Thirst Satiation Signals

Vineet Augustine,^{1,3} Haruka Ebisu,^{1,3} Yuan Zhao,¹ Sangjun Lee,¹ Brittany Ho,¹ Grace O. Mizuno,² Lin Tian,² and Yuki Oka^{1,4,*}

¹Division of Biology and Biological Engineering, California Institute of Technology, Pasadena, CA 91125, USA

²Department of Biochemistry and Molecular Medicine, University of California, Davis, Davis, CA 95616, USA

³These authors contributed equally

⁴Lead Contact

*Correspondence: yoka@caltech.edu

<https://doi.org/10.1016/j.neuron.2019.04.039>

SUMMARY

For thirsty animals, fluid intake provides both satiation and pleasure of drinking. How the brain processes these factors is currently unknown. Here, we identified neural circuits underlying thirst satiation and examined their contribution to reward signals. We show that thirst-driving neurons receive temporally distinct satiation signals by liquid-gulping-induced oropharyngeal stimuli and gut osmolality sensing. We demonstrate that individual thirst satiation signals are mediated by anatomically distinct inhibitory neural circuits in the lamina terminalis. Moreover, we used an ultrafast dopamine (DA) sensor to examine whether thirst satiation itself stimulates the reward-related circuits. Interestingly, spontaneous drinking behavior but not thirst drive reduction triggered DA release. Importantly, chemogenetic stimulation of thirst satiation neurons did not activate DA neurons under water-restricted conditions. Together, this study dissected the thirst satiation circuit, the activity of which is functionally separable from reward-related brain activity.

INTRODUCTION

The timing and amount of water intake is strictly regulated by the brain for maintaining body fluid homeostasis (Augustine et al., 2018b; Gizowski and Bourque, 2018; Ichiki et al., 2019; McKinley and Johnson, 2004). Fluid imbalance, such as dehydration, is mainly detected by a forebrain structure, lamina terminalis (LT). Recent studies have pinpointed neural populations and the circuit organization in the LT that process the internal fluid information (Abbott et al., 2016; Allen et al., 2017; Augustine et al., 2018a; Betley et al., 2015; Leib et al., 2017; Matsuda et al., 2017; Nation et al., 2016; Oka et al., 2015). Emerging evidence suggests that drinking behavior rapidly affects the activity of thirst circuits prior to water absorption into the systemic circulation (Allen et al., 2017; Augustine et al., 2018a; Gizowski et al., 2016; Mandelblat-Cerf et al., 2015; Thrasher et al., 1981; Zim-

merman et al., 2016). For example, thirst-related neurons in the LT receive rapid inhibitory signals with the onset of fluid ingestion. We have reported that an inhibitory circuit, involving MnPO neurons that express glucagon-like peptide 1 receptor (MnPO^{GLP1r} neurons), is activated by liquid gulping behavior (Augustine et al., 2018a). Once activated, these neurons monosynaptically inhibit thirst neurons in the subfornical organ (SFO). In addition to these gulping-induced signals, thirst neurons receive another satiation signal by postoral osmolality (hypotonicity) sensing, the neural basis of which remains unknown.

Besides satiation factors, water serves as reward for dehydrated animals and reinforces motivated ingestive behavior (Berridge, 2004; Epstein, 1982). Previous studies demonstrated that water intake activates the reward circuits in an internal-state-dependent manner (Bayer and Glimcher, 2005; Fortin and Roitman, 2018; Lin et al., 2014). Although reward and satiation are key factors that control ingestive behaviors, how these signals interact in the brain is unknown. In this study, we use optical recording of neural activity and dopamine (DA) release to examine the representation of thirst satiation signals in the reward-related circuit.

RESULTS

Liquid Gulping and Gut Osmolality Sensing Transmit Temporally Distinct Thirst Satiation Signals to the Brain

Thirst neurons in the LT receive inhibitory signals from both oropharyngeal and gastrointestinal areas associated with water intake (Augustine et al., 2018a; Zimmerman et al., 2019). To characterize individual thirst satiation signals, we combined calcium recording *in vivo* with intragastric (IG) infusion in awake-behaving animals. We first transduced adeno-associated virus (AAV) encoding Cre-dependent GCaMP6s in neuronal nitric oxide synthase (nNOS)-positive SFO neurons (SFO^{nNOS}) using nNOS-Cre transgenic mice (Figure S1A). This procedure was followed by intragastric surgery to implant a gastric cannula for fluid infusion (Ueno et al., 2012; Figures 1A and S1B). Oral consumption of water rapidly quenched the activity of SFO^{nNOS} neurons (<10 s). Similar levels of suppression were observed by IG infusion of water. However, the onset of suppression was significantly slower (>50 s; Figures 1B and 1C). These results indicate that oropharyngeal and gastrointestinal signals transmit independent inhibitory inputs to the thirst circuit. We next examined

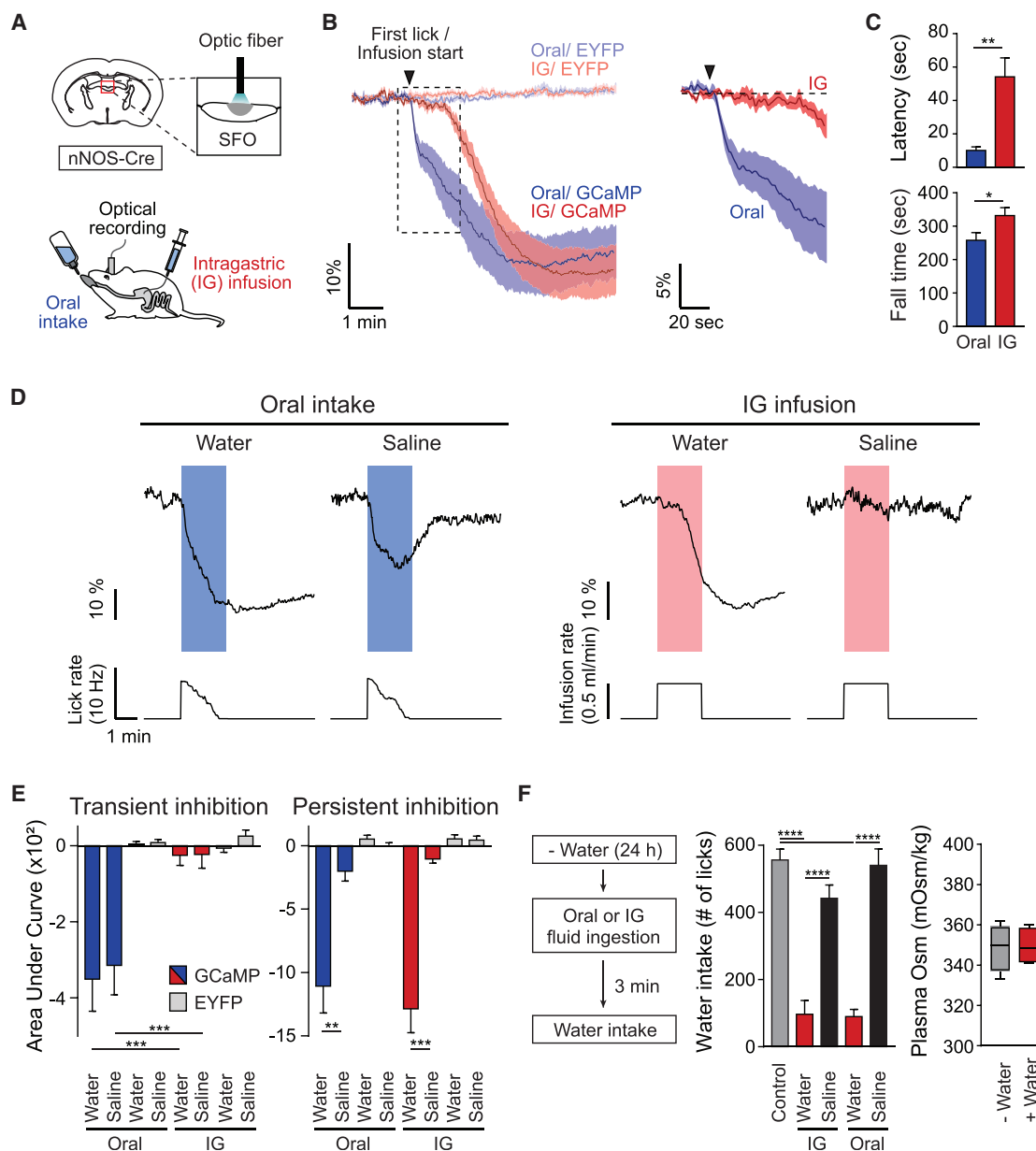


Figure 1. Thirst Circuits Receive Temporally Distinct Inhibitory Signals after Water Intake

(A) A diagram of optical recording of GCaMP6s signals from SFO^{nNOS} neurons. Fluid was given either orally or via IG infusion.

(B) Temporally distinct inhibition of SFO^{nNOS} neurons by ad lib oral intake or IG infusion of water (0.5 mL/min for 2 min; n = 8 mice for GCaMP6s; n = 4 and 6 mice for enhanced yellow fluorescent protein (EYFP) for oral and IG administration, respectively).

(C) IG water infusion induced significantly slower onset of inhibition compared to oral water intake (latency). Fall time is defined as the time to maximum inhibition from first lick or infusion onset (n = 8 mice for GCaMP6s).

(D) Representative traces of calcium dynamics during oral intake or IG infusion of water and saline (1 out of 8 mice). Lick and infusion rates are indicated below calcium traces.

(E) Quantified responses of SFO^{nNOS} neurons. Signals were quantified during (transient) and after (persistent) liquid ingestion or infusion; n = 8 mice for GCaMP6s; n = 6 mice for EYFP.

(F) Drinking-induced satiation after oral or IG water administration. Animals were given access to water after oral intake or IG infusion (0.5 mL/min) of fluid for 2 min. Water consumption was measured for 10 min (left, n = 11 mice for control [no pre-ingestion] and for pre-IG; n = 7 mice for pre-oral). Note that the systemic osmolality was unchanged after oral water intake (right, n = 4 mice).

*p < 0.05, **p < 0.01, ***p < 0.001, and ****p < 0.0001 by two-tailed paired t test; two-way repeated-measures ANOVA (Bonferroni's multiple comparisons) or one-way ANOVA (Tukey's multiple comparisons). Data are presented as mean ± SEM. Boxplots show median, quartiles (boxes), and range (whiskers). See also Figure S1.

the effect of fluid tonicity on the inhibitory signals. Oral intake of water or isotonic saline suppressed SFO^{nNOS} neural activity, whereas the inhibition by saline was transient. By contrast, IG infusion of isotonic fluids exhibited no inhibitory effect (Figures 1D, 1E, and S1C–S1F). Importantly, IG water infusion drastically suppressed SFO^{nNOS} neurons as well as subsequent water consumption (Figures 1D–1F). Collectively, these data show that (1) gut osmolality changes induce persistent pre-absorptive thirst satiation and (2) oropharyngeal stimulation by drinking action is not required for osmolality-induced satiation signals.

GLP1r-Positive SFO Neurons Mediate Thirst Satiation Signals by Gut Osmolality Change

We have recently shown that GLP1r-positive MnPO neurons (MnPO^{GLP1r}) mediate rapid inhibitory signals evoked by liquid gulping action regardless of osmolality (Augustine et al., 2018a). However, the neural substrates that encode osmolality-induced satiation have not been characterized. Because optogenetic activation of the SFO GABAergic population strongly suppressed water intake in thirsty animals (Oka et al., 2015), we suspected that these inhibitory neurons may be involved in osmolality-induced satiation signals. Histological analysis revealed that a majority of GABAergic SFO neurons expressed GLP1r (SFO^{GLP1r}; Figures 2A and S2A). Consistent with previous publication (Oka et al., 2015), SFO^{GLP1r} neurons were distinct from thirst-driving SFO^{nNOS} neurons, and optogenetic activation of ChR2-expressing SFO^{GLP1r} neurons drastically suppressed water intake in water-deprived animals (Figures 2B and S2B–S2D). Our electrophysiological experiments confirmed that SFO^{GLP1r} neurons send monosynaptic inhibitory inputs to SFO^{GLP1r}-negative (presumably SFO^{nNOS}) neurons (Figures 2C and S2E), suggesting direct local inhibition within the SFO. We note that the application of a GLP1r agonist did not change acute firing rate (Figure S2F).

We next tested whether SFO^{GLP1r} neurons are involved in osmolality-induced inhibition of thirst neurons using fiber photometry. Similar to MnPO^{GLP1r} neurons (Augustine et al., 2018a), SFO^{GLP1r} neurons were strongly activated upon water ingestion (Figure 2D). However, compared to MnPO^{GLP1r} neurons, SFO^{GLP1r} neurons showed significantly slower calcium dynamics (Figure 2D). Indeed, the activation of SFO^{GLP1r} neurons was observed toward the end of licking episodes and lasted for several minutes. Because ingested water stimulates oropharyngeal and gastrointestinal areas in a sequential manner, our results suggest that MnPO^{GLP1r} neurons transmit oropharyngeal-induced satiation, and SFO^{GLP1r} neurons mediate satiation signals originated from gut osmolality sensing (Figure 2E).

If this model is correct, we expect that SFO^{GLP1r} neurons should be selectively activated by hypo-osmotic stimuli in the gut. To directly test this, we recorded neural activity of SFO^{GLP1r} neurons upon fluid administration via the oral or IG route. These neurons were strongly activated by oral water intake, but not by silicone oil or isotonic saline (Figures 3A, 3B, and S3A–S3C). Similarly, ingestion of Ensure under hungry conditions did not activate this population (Figure 3B, right). Moreover, this activation did not require oropharyngeal stimulation because IG infusion of water induced similar activation of SFO^{GLP1r} neurons (Figures 3C and S3D). Together, these results demonstrate that

SFO^{GLP1r} neurons represent gut osmolality changes, which in turn transmit satiation signals to SFO^{nNOS}-positive thirst neurons through monosynaptic inhibition.

We next examined the significance of SFO^{GLP1r} neurons in regulating water intake using an inhibitory opsin, stGtACR2 (Mahn et al., 2018). In the presence of blue light, neural firing was strongly inhibited (Figure S3E) and animals drank significantly more water compared to no-light conditions (Figure 3D). By contrast, saline intake was not affected by photoinhibition. These results support our model that SFO^{GLP1r} neurons transmit osmolality signals to SFO^{nNOS} neurons.

Thirst Satiation Is Functionally Separable from Drinking-Associated Dopamine Release

For thirsty animals, water intake is both satiating and rewarding. According to drive-reduction theory, satiation should be the driving factor for drinking. It is, however, unknown whether thirst satiation directly serves as reward signals. Recent development of genetically encoded neuromodulator sensors allows us to examine real-time activity of the reward circuit during ingestive behaviors (Patriarchi et al., 2018; Sun et al., 2018). Given the neural basis of thirst satiation, we next employed a dopamine sensor, dLight (Patriarchi et al., 2018), to ask how the reward circuit responds to thirst satiation signals. We injected AAV-hSyn-dLight1.3 in the dorsal part of the nucleus accumbens medial shell (NAc) and implanted an optic fiber (400 μ m diameter) for recording DA release as fluorescence changes (Figures 4A and S4A). In accordance with recent studies (Brischoux et al., 2009; Cohen et al., 2012; Patriarchi et al., 2018), DA release rapidly increased in the NAc upon a rewarding stimulus (Ensure intake) and decreased upon an aversive stimulus (footshock; Figure 4B). During spontaneous drinking, rapid and sustained DA release in the NAc was observed for both water and saline (Figures 4C, 4D, left, and S4B). In sharp contrast, IG infusion of water, saline, or air had no effect on DA release (Figures 4C, 4D, and S4B). We observed similar results from presynaptic activity of tyrosine hydroxylase (TH)-positive neurons of the ventral tegmental area (VTA) or DA release in the dorsal striatum (Figures S4C–S4E). These results demonstrate that quenching thirst neurons (and thus, thirst drive reduction) is not sufficient to activate the reward circuit. We further examined whether stimulation of thirst satiation signals evokes DA release. To this end, we expressed an excitatory designer receptor exclusively activated by designer drugs (DREADD; hM3Dq) in SFO^{GLP1r}/MnPO^{GLP1r} neurons while infecting dLight1.3 in NAc neurons. This experimental setting allowed us to activate thirst satiation neurons chemogenetically while recording DA release in the same animals (Figure 4E). As a behavioral control, we confirmed that activation of hM3Dq-expressing SFO^{GLP1r}/MnPO^{GLP1r} neurons by clozapine-N-oxide (CNO) drastically inhibited water intake in water-deprived animals (Figure 4F). In these animals, CNO injection had no effect on DA release (Figure 4G). Importantly, consistent with optical recording above, IG water infusion failed to reinforce the lever-press behavior in water-deprived animals (Figures 4H and S4F). Taken together, this study provides important functional implications for satiation and reward processing in the mammalian brain. First, thirst satiation signals mediated by MnPO^{GLP1r} and SFO^{GLP1r} neurons are functionally separable

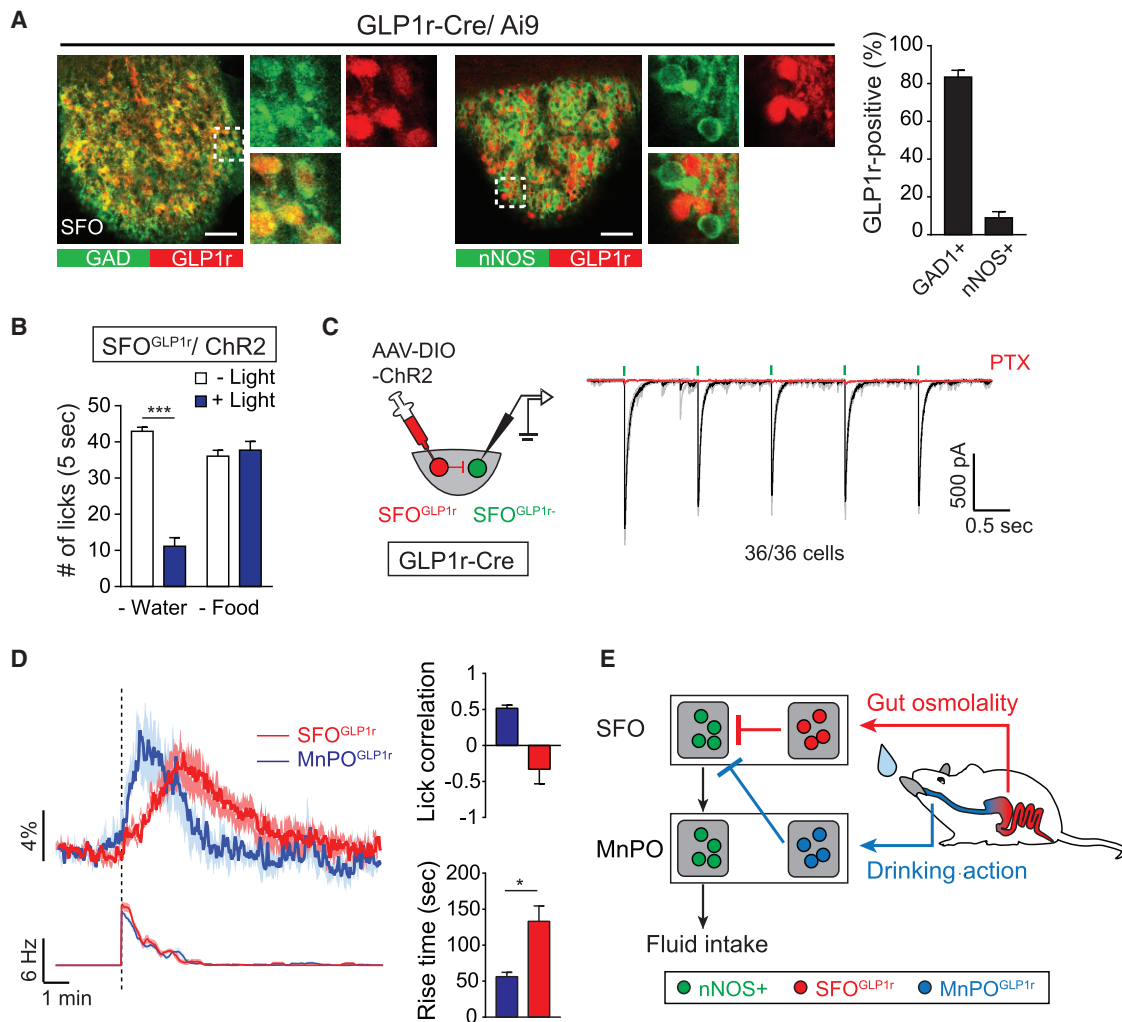


Figure 2. GLP1r-Positive SFO Neurons Monosynaptically Inhibit Thirst-Driving Neurons

(A) GLP1r is specifically expressed in GABAergic neurons of the SFO. Immunohistological staining shows that a majority of GLP1r-positive neurons (labeled by Ai9) overlapped with glutamic acid decarboxylase (GAD; left panels). These neurons did not overlap with glutamatergic nNOS-positive neurons (middle panels). Quantification of the percentage of GLP1r-positive neurons that coexpressed GAD or nNOS is shown ($n = 3$ mice; representative images are from 1 out of 3 mice). (B) Optogenetic stimulation of SFO^{GLP1r} neurons selectively suppresses water intake, but not liquid food intake ($n = 5$ mice). (C) The SFO^{GLP1r} → SFO^{non-GLP1r} monosynaptic connections. All GLP1r-negative neurons (36/36 cells) in the SFO received monosynaptic inhibitory inputs from SFO^{GLP1r} neurons.

(D) Two inhibitory populations in the LT exhibit temporally distinct response to drinking behavior. Calcium dynamics of SFO^{GLP1r} and MnPO^{GLP1r} neurons upon water drinking and lick rate (left) is shown. Quantification of calcium dynamics is shown. MnPO^{GLP1r} neurons have significantly faster activation kinetics compared to SFO^{GLP1r} neurons (right). MnPO^{GLP1r}, but not SFO^{GLP1r}, neurons have a positive correlation with lick timing ($n = 6$ mice). Rise time is defined as the time to maximum excitation from first lick. For MnPO^{GLP1r} neurons, we re-analyzed the data from the previous report (Augustine et al., 2018a).

(E) A possible model of thirst-quenching signals. Liquid gulping signals are mediated by MnPO^{GLP1r} neurons, which provide rapid and transient suppression of SFO^{nNOS} neurons. Subsequently, SFO^{GLP1r} neurons are activated by gastrointestinal hypo-osmotic stimuli to mediate slower inhibitory signals.

* $p < 0.05$; *** $p < 0.001$ by two-tailed paired or unpaired (Welch's correction) t test. Data are presented as mean \pm SEM. Scale bars, 50 μ m. See also Figure S2.

from DA release. Second, DA release is equally induced by water and saline drinking regardless of the homeostatic outcome.

DISCUSSION

Recent studies revealed genetically defined appetite circuits that regulate initiation of ingestive behaviors (Andermann and Lowell, 2017; Augustine et al., 2018b; Sternson and Eiselt, 2017).

Conversely, the mechanisms underlying ingestive termination are not well understood. In this study, we demonstrated that osmolality sensing in the gut induces persistent inhibition of thirst neurons in the SFO. We further show that gut osmolality change is mediated at least in part by a specific inhibitory population of the SFO: SFO^{GLP1r} neurons. We have shown that another inhibitory population, MnPO^{GLP1r}, transmits gulping-induced transient inhibition to thirst neurons. Thus, despite the lack of

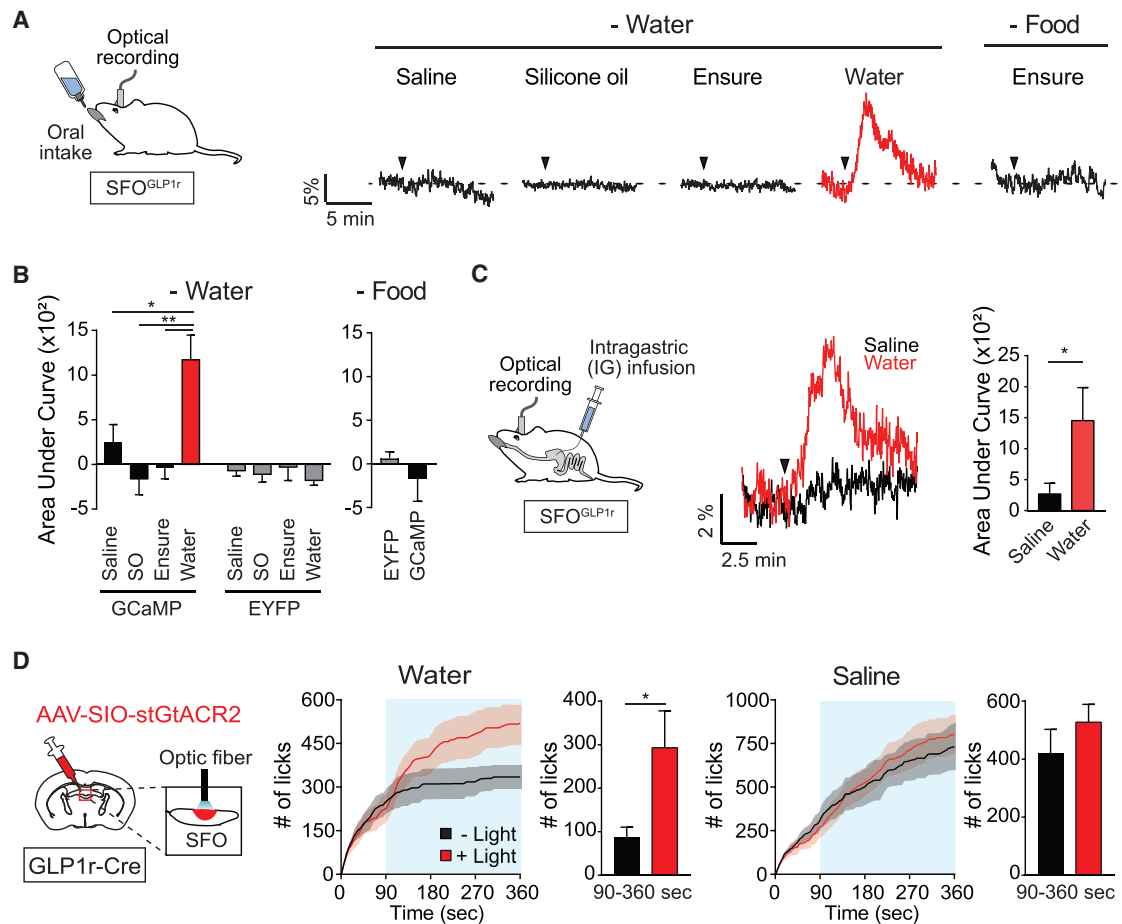


Figure 3. SFO^{GLP1r} Neurons Are Activated by Hypo-osmotic Stimuli in the Gut

(A) Representative traces showing calcium responses of SFO^{GLP1r} neurons upon ingestion of different fluids. SFO^{GLP1r} neurons were selectively activated by water, but not by other fluids. Black triangles indicate the onset of licking (1 out of 6 mice).

(B) Quantification of responses of GCaMP6s and EYFP signals during 5 min after the first lick ($n = 6$ and 3 mice for GCaMP6s for water and food restriction, respectively, and $n = 6$ mice for EYFP). SO, silicone oil.

(C) Responses of SFO^{GLP1r} neurons upon intragastric fluid infusion. A diagram of IG infusion and fiber photometry is shown (left panel). Representative traces are shown for IG water (red) or isotonic saline (black) infusion. A total of 1 mL (0.5 mL/min) of water or saline was infused. Black triangle indicates the onset of infusion (middle panel, traces are from 1 of 5 mice). Quantification of calcium responses to water or isotonic saline is shown (right panel, $n = 5$ mice).

(D) Optogenetic inhibition of SFO^{GLP1r} neurons selectively increases water intake, but not isotonic saline intake. SFO neurons of GLP1r-Cre mice were infected with AAV-SIO-stGtACR2. Continuous illumination was performed from 90 to 360 s (blue shaded area; $n = 5$ mice).

* $p < 0.05$ and ** $p < 0.01$ by two-tailed paired t test or one-way repeated-measures ANOVA (Dunnett's multiple comparisons). Data are presented as mean \pm SEM. See also Figure S3.

single-cell information in photometry recording, our results indicate that the LT contains two distinct thirst satiation pathways that are activated at distinct kinetics after the drinking onset. What is the functional significance of redundant thirst satiation signals? Interestingly, silencing SFO^{GLP1r} neurons increased hypo-osmotic fluid intake (Figures 3D and S3E), and silencing MnPO^{GLP1r} neurons augmented intake of non-hypo-osmotic liquid (Augustine et al., 2018a). A potential model is that the initial thirst satiation signals by MnPO^{GLP1r} neurons prevent animals from excessive fluid intake in general, and the slower satiation by SFO^{GLP1r} neurons ensures that animals have drunk hypo-osmotic fluids that are rehydrating (Booth, 1991; Figure 2E). How thirst satiation signals are transmitted from the periphery to the

brain is currently unclear (Kim et al., 2018). The gut-to-brain signaling may require afferent neural pathways (Zimmerman et al., 2019) or hormonal signaling.

Nutrient ingestion induces both satiation and satisfaction (Lee et al., 2019; Rossi and Stuber, 2018). It has been shown that postingestive nutrient signals after feeding stimulate DA release in the brain (Figure S4G; Han et al., 2018; Ren et al., 2010). But few studies to date have investigated the interaction of satiation and reward processing for thirst regulation. We have shown that DA release is exclusively induced by drinking behavior regardless of liquid type. Notably, suppression of thirst neurons by IG water infusion or stimulation of GLP1r-positive LT neurons did not induce robust DA release. These

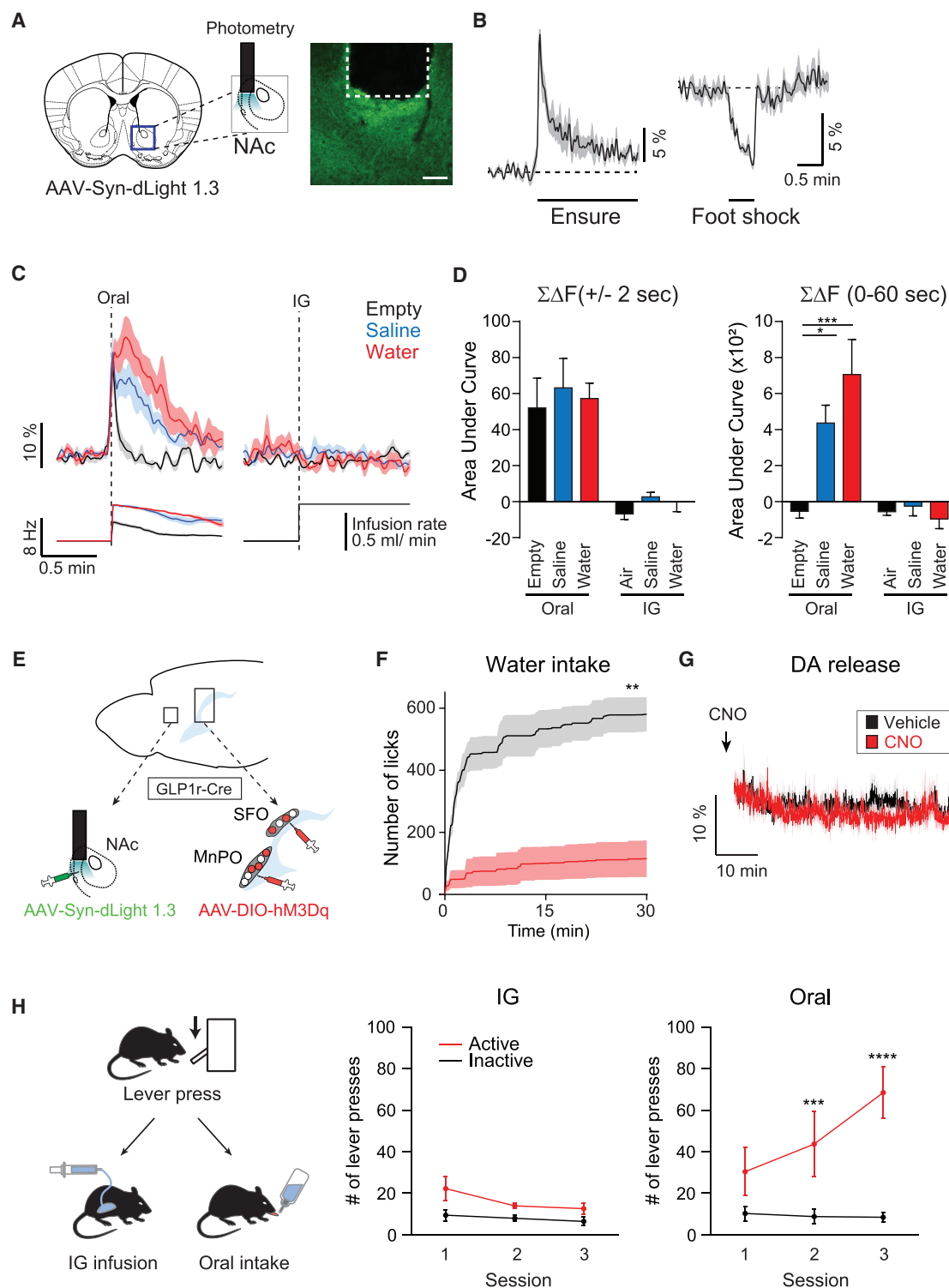


Figure 4. Activity of the Reward Circuits Is Separable from Thirst Satiation Signals

(A) A diagram of optical recording of DA release by dLight1.3. A representative image of dLight expression is shown.

(B) DA release is induced by appetitive (Ensure) stimulus and suppressed by aversive (footshock) stimulus (n = 7 mice).

(C) dLight fluorescence changes are shown during oral ad lib intake and IG infusion (n = 7 mice). Spontaneous drinking induced robust DA release in the NAc compared to empty control regardless of liquid type (left). For empty control experiments, DA release was observed transiently prior to lick due to reward expectation. By contrast, IG infusion of fluid had no effect on DA release (right, n = 7 mice).

(legend continued on next page)

results explain the previous findings that non-oral water ingestion (e.g., IG or intravenous water infusion) is much less rewarding as compared to oral drinking (McFarland, 1969; Nicolaidis and Rowland, 1974). From the functional perspective of DA neurons, this study demonstrates that reinforcement learning for water intake requires peripheral signals associated with drinking, but not the reduction of appetite per se. Nevertheless, the valence of water is highly affected by internal state, suggesting that homeostatic signals modulate reward processing. Identifying neural substrates that integrate interoceptive and reward signals will provide insights into appetite and behavioral regulations in the brain.

STAR★METHODS

Detailed methods are provided in the online version of this paper and include the following:

- KEY RESOURCES TABLE
- CONTACT FOR REAGENT AND RESOURCE SHARING
- EXPERIMENTAL MODEL AND SUBJECT DETAILS
 - Animals
- METHOD DETAILS
 - Surgery
 - Optogenetic manipulation
 - Chemogenetic manipulation
 - Behavioral assays
 - Long-term access assays
 - Brief access assays
 - Lever-pressing for water reward
 - Fiber photometry
 - dLight1.3b sensitivity experiments
 - Histology
 - Plasma osmolality measurements
 - Slice electrophysiology
- QUANTIFICATION AND STATISTICAL ANALYSIS

SUPPLEMENTAL INFORMATION

Supplemental Information can be found online at <https://doi.org/10.1016/j.neuron.2019.04.039>.

ACKNOWLEDGMENTS

We thank Drs. Joshua Berke and Anne Andrews and the members of the Oka laboratory for helpful discussion and comments. This work was supported by startup funds from the President and Provost of California Institute of Technology and the Biology and Biological Engineering Division of California Institute of Technology. Y.O. is also supported by the Searle Scholars Program, the

Mallinckrodt Foundation, the McKnight Foundation, the Klingenstein-Simons Foundation, and NIH (R01NS109997 and R56MH113030). H.E. is supported by the Uehara Memorial Foundation and Japan Society for the Promotion of Science.

AUTHOR CONTRIBUTIONS

V.A., H.E., and Y.O. conceived the research program and designed experiments. V.A. and H.E. carried out the experiments and analyzed the data with help from S.L. and B.H. Y.Z. performed all slice patch-clamp recordings. L.T. and G.O.M. provided dLight1.3 viruses and performed *in vitro* experiments. V.A., H.E., and Y.O. wrote the paper. Y.O. supervised the entire work.

DECLARATION OF INTERESTS

The authors declare no competing interests.

Received: January 15, 2019

Revised: March 27, 2019

Accepted: April 26, 2019

Published: May 29, 2019

REFERENCES

- Abbott, S.B., Machado, N.L., Geerling, J.C., and Saper, C.B. (2016). Reciprocal control of drinking behavior by median preoptic neurons in mice. *J. Neurosci.* 36, 8228–8237.
- Allen, W.E., DeNardo, L.A., Chen, M.Z., Liu, C.D., Loh, K.M., Fenno, L.E., Ramakrishnan, C., Deisseroth, K., and Luo, L. (2017). Thirst-associated pre-optic neurons encode an aversive motivational drive. *Science* 357, 1149–1155.
- Andermann, M.L., and Lowell, B.B. (2017). Toward a wiring diagram understanding of appetite control. *Neuron* 95, 757–778.
- Augustine, V., Gokce, S.K., Lee, S., Wang, B., Davidson, T.J., Reimann, F., Gribble, F., Deisseroth, K., Lois, C., and Oka, Y. (2018a). Hierarchical neural architecture underlying thirst regulation. *Nature* 555, 204–209.
- Augustine, V., Gokce, S.K., and Oka, Y. (2018b). Peripheral and central nutrient sensing underlying appetite regulation. *Trends Neurosci.* 41, 526–539.
- Bayer, H.M., and Glimcher, P.W. (2005). Midbrain dopamine neurons encode a quantitative reward prediction error signal. *Neuron* 47, 129–141.
- Berridge, K.C. (2004). Motivation concepts in behavioral neuroscience. *Physiol. Behav.* 81, 179–209.
- Betley, J.N., Xu, S., Cao, Z.F.H., Gong, R., Magnus, C.J., Yu, Y., and Sternson, S.M. (2015). Neurons for hunger and thirst transmit a negative-valence teaching signal. *Nature* 521, 180–185.
- Booth, D.J.R.A.D. (1991). Thirst: Physiological and Psychological Aspects (Springer-Verlag).
- Brischoux, F., Chakraborty, S., Brierley, D.I., and Ungless, M.A. (2009). Phasic excitation of dopamine neurons in ventral VTA by noxious stimuli. *Proc. Natl. Acad. Sci. USA* 106, 4894–4899.
- Cohen, J.Y., Haesler, S., Vong, L., Lowell, B.B., and Uchida, N. (2012). Neuron-type-specific signals for reward and punishment in the ventral tegmental area. *Nature* 482, 85–88.

(D) Quantified data of dLight responses during 4 s around the first lick (left) or 60 s (right) after the first lick or IG infusion (n = 7 mice).

(E) A schematic for activating thirst satiation circuits in the LT by hM3Dq while measuring DA release in the NAc by dLight1.3.

(F) Chemogenetic stimulation of SFO^{GLP1r} and MnPO^{GLP1r} neurons attenuates water intake under dehydrated conditions (n = 6 mice).

(G) By contrast, the same stimulation paradigm did not induce DA release (n = 6 mice).

(H) A diagram of operant task. Mice were initially trained to associate lever press and water reward. After extinction sessions (see Figure S4F), animals were subjected to reinstatement paradigms with either IG or oral water reward (left). In IG sessions, animals received water through a gastric catheter on an FR3 schedule (middle). In oral sessions, the same amount of water reward was provided through a spout (right, n = 6 mice). Only oral water intake efficiently reinforced lever press behavior.

*p < 0.05, **p < 0.01, ***p < 0.001, and ****p < 0.0001 by two-tailed paired t test; one-way repeated-measures ANOVA (Dunnett's multiple comparisons) or two-way repeated-measures ANOVA (Bonferroni's multiple comparisons). Data are presented as mean ± SEM. Scale bar, 50 μm. See also Figure S4.

- Epstein, A.N. (1982). The physiology of thirst. In *The Physiological Mechanisms of Motivation*, D.W. Pfaff, ed. (Springer New York).
- Fortin, S.M., and Roitman, M.F. (2018). Challenges to body fluid homeostasis differentially recruit phasic dopamine signaling in a taste-selective manner. *J. Neurosci.* 38, 6841–6853.
- Gipson, C.D., Reissner, K.J., Kupchik, Y.M., Smith, A.C., Stankeviciute, N., Hensley-Simon, M.E., and Kalivas, P.W. (2013). Reinstatement of nicotine seeking is mediated by glutamatergic plasticity. *Proc. Natl. Acad. Sci. USA* 110, 9124–9129.
- Gizowski, C., and Bourque, C.W. (2018). The neural basis of homeostatic and anticipatory thirst. *Nat. Rev. Nephrol.* 14, 11–25.
- Gizowski, C., Zaelzer, C., and Bourque, C.W. (2016). Clock-driven vasopressin neurotransmission mediates anticipatory thirst prior to sleep. *Nature* 537, 685–688.
- Han, W., Tellez, L.A., Perkins, M.H., Perez, I.O., Qu, T., Ferreira, J., Ferreira, T.L., Quinn, D., Liu, Z.W., Gao, X.B., et al. (2018). A neural circuit for gut-induced reward. *Cell* 175, 665–678.e23.
- Ichiki, T., Augustine, V., and Oka, Y. (2019). Neural populations for maintaining body fluid balance. *Curr. Opin. Neurobiol.* 57, 134–140.
- Kim, K.S., Seeley, R.J., and Sandoval, D.A. (2018). Signalling from the periphery to the brain that regulates energy homeostasis. *Nat. Rev. Neurosci.* 19, 185–196.
- Lee, S., Augustine, V., Zhao, Y., Ebisu, H., Ho, B., Kong, D., and Oka, Y. (2019). Chemosensory modulation of neural circuits for sodium appetite. *Nature* 568, 93–97.
- Leib, D.E., Zimmerman, C.A., Poormoghaddam, A., Huey, E.L., Ahn, J.S., Lin, Y.C., Tan, C.L., Chen, Y., and Knight, Z.A. (2017). The forebrain thirst circuit drives drinking through negative reinforcement. *Neuron* 96, 1272–1281.e4.
- Lin, S., Oswald, D., Chandra, V., Talbot, C., Huetteroth, W., and Waddell, S. (2014). Neural correlates of water reward in thirsty *Drosophila*. *Nat. Neurosci.* 17, 1536–1542.
- Mahn, M., Gibor, L., Patil, P., Cohen-Kashi Malina, K., Oring, S., Printz, Y., Levy, R., Lampl, I., and Yizhar, O. (2018). High-efficiency optogenetic silencing with soma-targeted anion-conducting channelrhodopsins. *Nat. Commun.* 9, 4125.
- Mandelblat-Cerf, Y., Ramesh, R.N., Burgess, C.R., Patella, P., Yang, Z., Lowell, B.B., and Andermann, M.L. (2015). Arcuate hypothalamic AgRP and putative POMC neurons show opposite changes in spiking across multiple timescales. *eLife* 4, e07112.
- Matsuda, T., Hiyama, T.Y., Niimura, F., Matsusaka, T., Fukamizu, A., Kobayashi, K., Kobayashi, K., and Noda, M. (2017). Distinct neural mechanisms for the control of thirst and salt appetite in the subfornical organ. *Nat. Neurosci.* 20, 230–241.
- McFarland, D. (1969). Separation of satiating and rewarding consequences of drinking. *Physiol. Behav.* 4, 987–989.
- McKinley, M.J., and Johnson, A.K. (2004). The physiological regulation of thirst and fluid intake. *News Physiol. Sci.* 19, 1–6.
- Nation, H.L., Nicoleau, M., Kinsman, B.J., Browning, K.N., and Stocker, S.D. (2016). DREADD-induced activation of subfornical organ neurons stimulates thirst and salt appetite. *J. Neurophysiol.* 115, 3123–3129.
- Nicolaïdis, S., and Rowland, N. (1974). Long-term self-intravenous “drinking” in the rat. *J. Comp. Physiol. Psychol.* 87, 1–15.
- Oka, Y., Ye, M., and Zuker, C.S. (2015). Thirst driving and suppressing signals encoded by distinct neural populations in the brain. *Nature* 520, 349–352.
- Patriarchi, T., Cho, J.R., Merten, K., Howe, M.W., Marley, A., Xiong, W.H., Folk, R.W., Broussard, G.J., Liang, R., Jang, M.J., et al. (2018). Ultrafast neuronal imaging of dopamine dynamics with designed genetically encoded sensors. *Science* 360, eaat4422.
- Ren, X., Ferreira, J.G., Zhou, L., Shammah-Lagnado, S.J., Yeckel, C.W., and de Araujo, I.E. (2010). Nutrient selection in the absence of taste receptor signaling. *J. Neurosci.* 30, 8012–8023.
- Rossi, M.A., and Stuber, G.D. (2018). Overlapping brain circuits for homeostatic and hedonic feeding. *Cell Metab.* 27, 42–56.
- Sternson, S.M., and Eiselt, A.K. (2017). Three pillars for the neural control of appetite. *Annu. Rev. Physiol.* 79, 401–423.
- Sun, F., Zeng, J., Jing, M., Zhou, J., Feng, J., Owen, S.F., Luo, Y., Li, F., Wang, H., Yamaguchi, T., et al. (2018). A genetically encoded fluorescent sensor enables rapid and specific detection of dopamine in flies, fish, and mice. *Cell* 174, 481–496.e19.
- Thrasher, T.N., Nistal-Herrera, J.F., Keil, L.C., and Ramsay, D.J. (1981). Satiety and inhibition of vasopressin secretion after drinking in dehydrated dogs. *Am. J. Physiol.* 240, E394–E401.
- Ueno, A., Lazaro, R., Wang, P.Y., Higashiyama, R., Machida, K., and Tsukamoto, H. (2012). Mouse intragastric infusion (iG) model. *Nat. Protoc.* 7, 771–781.
- Zimmerman, C.A., Lin, Y.C., Leib, D.E., Guo, L., Huey, E.L., Daly, G.E., Chen, Y., and Knight, Z.A. (2016). Thirst neurons anticipate the homeostatic consequences of eating and drinking. *Nature* 537, 680–684.
- Zimmerman, C.A., Huey, E.L., Ahn, J.S., Beutler, L.R., Tan, C.L., Kosar, S., Bai, L., Chen, Y., Corpuz, T.V., Madisen, L., et al. (2019). A gut-to-brain signal of fluid osmolarity controls thirst satiation. *Nature* 568, 98–102.

STAR★METHODS

KEY RESOURCES TABLE

REAGENT or RESOURCE	SOURCE	IDENTIFIER
Antibodies		
Rabbit monoclonal anti-GAD65+GAD67	Abcam	Cat#Ab183999
Rabbit polyclonal anti-Nos1	Santa Cruz	Cat#sc-648; RRID: AB_630935
Chicken polyclonal anti-GFP	Abcam	Cat#ab13970; RRID: AB_300798
Bacterial and Virus Strains		
AAV2-Ef1a-DIO-eYFP	UNC Vector Core	N/A
AAV2-Ef1a-DIO-ChR2-eYFP	UNC Vector Core	N/A
AAV1-hSyn1-flex-GCaMP6s-WPRE-SV40	Penn Vector Core, Addgene	Cat#100845-AAV1
AAV9-hSyn-dLight1.3	Dr. Lin Tian (UC, Davis)	N/A
AAV2-hSyn-DIO-hM3D(Gq)-mCherry	UNC Vector Core	N/A
AAV1-hSyn1-SIO-stGtACR2-FusionRed (diluted 10 times in PBS before injection)	Dr. David Anderson (Caltech)	N/A
Chemicals, Peptides, and Recombinant Proteins		
Silicone Oil	Sigma-Aldrich	378348
Exendin-4	Sigma-Aldrich	E7144
Clozapine N-oxide (CNO)	Sigma-Aldrich	C0832
D-Mannitol	Sigma-Aldrich	M9647
0.9% Sodium Chloride, USP	Hospira	NDC 0409-4888-02
Ensure	Abbott	N/A
20% Intra-lipid	Sigma-Aldrich	I141
Glucose	Macron	4912-12
Blue dye	Butler's	N/A
Experimental Models: Organisms/Strains		
Mouse: wild-type (C57BL/6J)	The Jackson Laboratory	Strain#000664; RRID: IMSR_JAX:000664
Mouse: Nos1-Cre knockin (B6.129-Nos1 ^{tm1(cre)Mgm} /J)	The Jackson Laboratory	Strain# 017526; RRID: IMSR_JAX:017526
Mouse: Ai75D (B6.Cg-Gt(ROSA) 26Sor ^{tm75.1(CAG-tdTomato*)Hze} /J)	The Jackson Laboratory	Strain# 025106; RRID: IMSR_JAX:025106
Mouse: Ai9 (B6.Cg-Gt(ROSA) 26Sor ^{tm9(CAG-tdTomato)Hze} /J)	The Jackson Laboratory	Strain# 007909; RRID: IMSR_JAX: 007909
Mouse: Ai3 (B6.Cg-Gt(ROSA) 26Sor ^{tm3(CAG-EYFP)Hze} /J)	The Jackson Laboratory	Strain# 007903; RRID: IMSR_JAX: 007903
GLP1r-cre	Dr. Fiona Gribble (University of Cambridge)	N/A
TH-Cre	Dr. Viviana Gradinaru (Caltech)	N/A
Software and Algorithms		
MATLAB R2016a/2017b	MathWorks	N/A
Prism 7/8	GraphPad	N/A
Photoshop CS6/CC	Adobe	N/A
Illustrator CS5/CC	Adobe	N/A
LASX	Leica	N/A
Office 2016	Microsoft	N/A

CONTACT FOR REAGENT AND RESOURCE SHARING

Further information and requests for resources and reagents should be directed to and will be fulfilled on reasonable request by the lead contact, Yuki Oka (yoka@caltech.edu).

EXPERIMENTAL MODEL AND SUBJECT DETAILS

Animals

All procedures followed animal care guidelines from NIH for the care and use of laboratory animals and California Institute of Technology Institutional Animal Care and Use Committee (1694–14). Animals used for experiment were at least 8 weeks of age. The following mice were purchased from the Jackson Laboratory: C57BL/6J, stock number 000664; Nos1-cre, stock number 017526; Ai75D, stock number 025106; Ai3, stock number 007903; Ai9, stock number 007909; GLP1r-cre and TH-Cre lines were provided by Dr. F. Gribble (Cambridge) and Dr. V. Gradinaru (Caltech), respectively. Mice were housed in temperature- and humidity-controlled rooms with a 13 h: 11 h light: dark cycle with ad libitum access to food and water except for specific depletion experiments (water, food). Male and female mice were used for experiments, and randomly assigned before surgery. Animals that underwent gastric catheter implantation surgery were singly-housed.

METHOD DETAILS

Surgery

Mice were anaesthetized with a mixture of ketamine (1 mg/mL) and xylazine (10 mg/mL) in isotonic saline, intraperitoneally (ip) injected at 10 μ L/g body weight. Ketoprofen was administered at 5 μ L/g body weight subcutaneously. The animal was then placed in a stereotaxic apparatus (Narishige Apparatus) with a heating pad. Surgery was performed as previously described ([Augustine et al., 2018a](#); [Oka et al., 2015](#)). In brief, the three-dimensional MRI coordinate system was used as a reference for the injection site coordinates. Viral constructs were injected using a microprocessor-controlled injection system (Nanoliter 2000, WPI) at 100 nL/min. The coordinates for SFO are AP: -4030 , ML: 0 , DV: -2550 (150–300 nL injection), MnPO are AP: -3100 , ML: 0 , DV: -4080 (100 nL injection) and -3800 (50 nL injection), dorsal part of the nucleus accumbens medial shell are AP: -2100 , ML: $+700$, DV: -4000 (500 nL injection), dorsal striatum are AP: -2400 , ML: $+1800$, DV: -4200 (500 nL injection), ventral tegmental area (VTA) are AP: -6000 , ML: $+1000$, DV: -4400 (200 nL injection).

For optogenetic experiments, implants were made with a 200 μ m fiber bundle (FT200EMT, Thorlabs) glued to a ceramic ferrule (CF230, Thorlabs). For photometry, a 400 μ m fiber bundle (FT400UMT, Thorlabs) and a ceramic ferrule (CF440, Thorlabs) were used. A fiber was implanted 300 μ m above (for optogenetic experiments) or inside the SFO, the dorsal part of the nucleus accumbens medial shell or the dorsal striatum (for photometry). Virus expression and implant position was verified after data collection.

For intragastric (IG) infusion, catheter construction and implantation closely followed as described previously ([Ueno et al., 2012](#)). IG catheters were custom made using silastic tubing (Dow Corning, 508-002), tygon tubing (Instech, BTPE-25) and pinport (Instech, PNP3F25-50) with a dead volume of approximately 13 μ L. IG surgery was performed after animals recovered from the initial optogenetic or photometry surgeries.

After surgery, animals were placed in a clean cage placed on a heating pad overnight. Animals were given at least 7 days post-surgery on antibiotics and Ibuprofen with ad lib food and water to allow complete recovery. Behavioral and histological experiments were then performed.

Optogenetic manipulation

For ChR2 photostimulation, 473 nm laser pulses (20ms, 20Hz) were delivered via an optic cable (MFP-FC-ZF, Doric Lenses) using a pulse generator (SYS-A310, WPI). The laser intensity was maintained at 10 mW at the tip of the fiber. For photoinhibition experiments, 473 nm light was continuously turned on with 7 mW intensity at the fiber tip.

Chemogenetic manipulation

For acute activation experiments, CNO dissolved in PBS was injected at 1 mg/kg body weight.

Behavioral assays

For water-restriction experiments, mice were provided with 1 mL of water daily. For food-restriction experiments, mice were provided with 0.5 pellets per 20 g of body weight daily. All assays were performed in home cages, an operant chamber or a modified lickometer as described previously ([Augustine et al., 2018a](#); [Oka et al., 2015](#)). In foot shock experiments ([Figure 4B](#)) animals were given a foot shock (0.3 mA) for 30 s.

Long-term access assays

After 24 h of water or food restriction, animals were acclimatized to the behavior chamber for 10–15 min. Animals were then given access to a bottle filled with water, isotonic saline, Ensure, or silicone oil for 2 min ([Figures 1D, 1E, S1C, S1D, and S1F](#)), or the entire

session (other data). For Figure 3D, no light was illuminated for the first 90 s of access. In the case of IG infusion experiments (Figures 1, 3C, 4C, S1, S3D, and S4B–S4E), animals were infused with water, isotonic saline, or isotonic mannitol for 2 min (0.5 mL/min) via gastric catheter using an infusion syringe pump (NE-300, New Era Pump Systems Inc). For Figure S4G, 45% glucose, 20% intralipid, isotonic saline, or water was infused at 50 μ L/min for 20 mins.

For Figure 1F, after 15 min of acclimatization, animals were given oral or IG administration of water or isotonic saline at 0.5 mL/min for 2 min. 3 min after administration, water consumption was measured for 10 min by a lickometer. Animals without fluid administration before the lick measurement were treated as controls.

For Figure 4F, 30 min after CNO/PBS (1 mg/kg) ip injection, water consumption was measured for 30 min by a lickometer after 24 h of water-restriction.

Brief access assays

Animals were subjected to water restriction, or food-deprivation (Figures 2B and S2D) for 24 h before behavioral experiments. In each 60 s trial, stimulation was started 10 s before water or Ensure presentation, and maintained until the end of the trial. The number of licks in a 5 s window following the first lick was analyzed. Animals were tested for six trials (3 each with light on/off) each, and the number of licks was averaged across trials.

Lever-pressing for water reward

The experimental method is adapted from a previous report (Gipson et al., 2013; McFarland, 1969). Mice were subjected to water deprivation for 24 h before each session. Sessions were done in an operant chamber equipped with two levers (active and inactive) and a lickometer (Med Associates). Animals were trained on FR1, followed by FR3 schedules to obtain water reward for 1 s from the lickometer (average 20 μ L/sec).

After training was completed, animals were tested under sated (control) and water-deprived conditions on FR3 schedule for 15 min. These test paradigms were followed by four extinction sessions for 15 min each. An empty water bottle was presented to animals during the extinction sessions. Animals were then subjected to FR3 reinstatement paradigms. As a reinforcer (reward), water was provided through the IG route (20 μ L) via a gastric catheter by a peristaltic pump (Minipuls 3, Gilson), or oral access. We analyzed whether IG or oral water intake reinforce lever press behavior after three training sessions for 15 min each (Figures 4H and S4F).

Fiber photometry

For all photometry assays, animals were acclimatized for 5 – 15 min in the chamber before stimuli were presented. Bulk fluorescence signals were collected using fiber photometry as previously described (Augustine et al., 2018a; Patriarchi et al., 2018). Signals were then extracted and subjected to a low-pass filter at 1.8 and 25 Hz for GCaMP and dLight respectively. A linear function was used to scale up the 405-nm channel signal to the 490-nm channel signal to obtain the fitted 405-nm signal. The resultant $\Delta F/F$ was calculated as (raw 490 nm signal – fitted 405 nm signal) / (fitted 405 nm signal). $\Delta F/F$ was then time-binned by a factor of 2.5 times the sampling frequency and down-sampled to 1 Hz. Data were detrended to account for photo-bleaching. For all sessions, the mean fluorescence for 4–5 min before the first lick, intragastric infusion start or CNO/saline ip injection was calculated and subtracted from the entire session. The licks from the lickometer were simultaneously recorded. The area under the curve (AUC) was quantified by integrating the baseline-subtracted fluorescence signals for 1 (for dLight) or 5 (for GCaMP of SFO^{GLP1r}) min after the start of the bout. For SFO^{nOS} neurons (Figures 1E, S1D, and S1E), AUCs were calculated for 50 s at two time points; after the start of administration (transient inhibition) and 80 s after the end of administration (persistent inhibition). Z-scores (Figure S4G) were calculated from the $\Delta F/F$ time-series signal (for 20 min after the start of intragastric infusion) by subtraction of mean and division by mean standard deviation of $\Delta F/F$ during saline intragastric infusion, calculated from all animals. This was to account for the signal variation for different stimuli infusion across animals.

dLight1.3b sensitivity experiments

For Figure S4A, AAV-cag-dLight1.3b was transfected in HEK293T cells. 48 h later, 293 cells were imaged continuously in HBSS while sequentially perfusing with 0.9% saline, 10 nM dopamine, HBSS washout, 10 nM dopamine and 5 nM DRD1 antagonist SCH 23390 as indicated.

Histology

Mice were anaesthetized with CO₂ and then transcardially perfused with PBS followed by 4% PFA in PBS (pH 7.4). The brain was dissected and fixed in 4% PFA at 4°C for overnight. Fixed brains were sectioned into 100 μ m coronal sections using a vibratome (Leica, VT-1000 s). For immunohistochemistry (IHC), brain sections were incubated in a blocking buffer (10% Donkey serum, 0.2% Triton-X) for 1–2 h. Sections were then incubated overnight with the following primary antibodies: rabbit anti-GAD65+GAD67 (1:500, Abcam, ab183999), rabbit anti-NOS1 (1:500, Santa Cruz, sc-648), chicken anti-GFP (1:1000, Abcam, ab13970). Sections were washed three times with PBS, then were incubated with secondary antibodies (1:500 dilutions, Jackson laboratory) in blocking buffer for 4 h. GAD65+GAD67 staining was performed without Triton-X.

Plasma osmolality measurements

After water deprivation for 24 h, trunk blood was collected in an EDTA coated tube, from wild-type mice before or 5 min after the water drinking onset. Plasma was then separated by centrifugation at 1500 g for 20 min. Plasma osmolality was measured using a vapor pressure osmometer (Vapro 5520).

Slice electrophysiology

Coronal sections containing SFO were obtained using a vibratome (VT-1000s, Leica) in ice-cold sucrose-aCSF (artificial cerebrospinal fluid) solution (in mM: Sucrose 213, KCl 2.5, NaH_2PO_4 1.2, NaHCO_3 25, glucose 10, MgSO_4 7, CaCl_2 1, at pH 7.3), and then incubated in normal aCSF (in mM: NaCl 124, KCl 2.5, NaH_2PO_4 1.2, NaHCO_3 24, glucose 25, MgSO_4 1, CaCl_2 2, bubbled with 95% O_2 /5% CO_2) at 34.5°C for 30 min. After that slices were held at room temperature until use.

For patch-clamp recording, slices were perfused with normal aCSF on an upright microscope (Examiner.D1, Zeiss). Electrical signals were filtered at 3kHz with Axon MultiClamp 700B (Molecular Devices) and collected at 20 kHz with Axon Digidata 1550A (Molecular Devices). For current clamp recordings, intracellular solution containing (in mM) K-gluconate 145, NaCl 2, KCl 4, HEPES 10, EGTA 0.2, Mg-ATP 4, Na-GTP 0.3 (pH 7.25) was used, while for voltage clamp whole-cell recordings, intracellular solution contained (in mM) CsCl 145, NaCl 2, HEPES 10, EGTA 0.2, QX-314 bromide 5, Mg-ATP 4, Na-GTP 0.3 (pH 7.25). In some experiments (Figures S2E and S2F), cell-attached loose-patch recordings (seal resistance, 20–80 M Ω) were performed.

For optogenetics experiments, light beam from an LED light source (X-Cite 120LED, Excelitas Technologies) was delivered through an optical filter (475/30). Light pulses (1–2 ms) were given 5 times at 1 Hz for 4 cycles in connectivity experiment (Figure 2C). To verify GABAergic connections, picrotoxin (100 μM) was applied through perfusion. Light was applied at 20 Hz for 5 s to show ChR2-induced neuronal firing in GLP1r+ cells (Figure S2C) and applied at 10 Hz for 20–30 s to verify the monosynaptic inhibition from GLP1r+ to GLP1r- cells (Figure S2E). To show inhibition by stGtACR2 (Figure S3E), light was continuously illuminated for 4.5 min to show the light-induced inhibition of GLP1r+ cells.

QUANTIFICATION AND STATISTICAL ANALYSIS

All statistical analyses were done using Prism (GraphPad). We either used a two-tailed paired/unpaired t test, one/two-way ANOVA depending on the experimental paradigm. * $p < 0.05$, ** $p < 0.01$, *** $p < 0.001$, **** $p < 0.0001$. Data sheets with the analysis of statistical tests from Prism reporting estimates of variance within each group, comparison of variances across groups are available on reasonable request. Viral expression and implant placement was verified by histology before animals were included in the analysis. While recording calcium dynamics of SFO^{nOS} neurons, animals with $\Delta F/F$ less than 10% by ip injection of 300 μL 2M NaCl were excluded from data analysis. These criteria were pre-established. No statistics to determine sample size, blinding or randomization methods were used. Data are presented as mean \pm sem unless otherwise mentioned.

Neuron, Volume 103

Supplemental Information

Temporally and Spatially Distinct

Thirst Satiation Signals

Vineet Augustine, Haruka Ebisu, Yuan Zhao, Sangjun Lee, Brittany Ho, Grace O. Mizuno, Lin Tian, and Yuki Oka

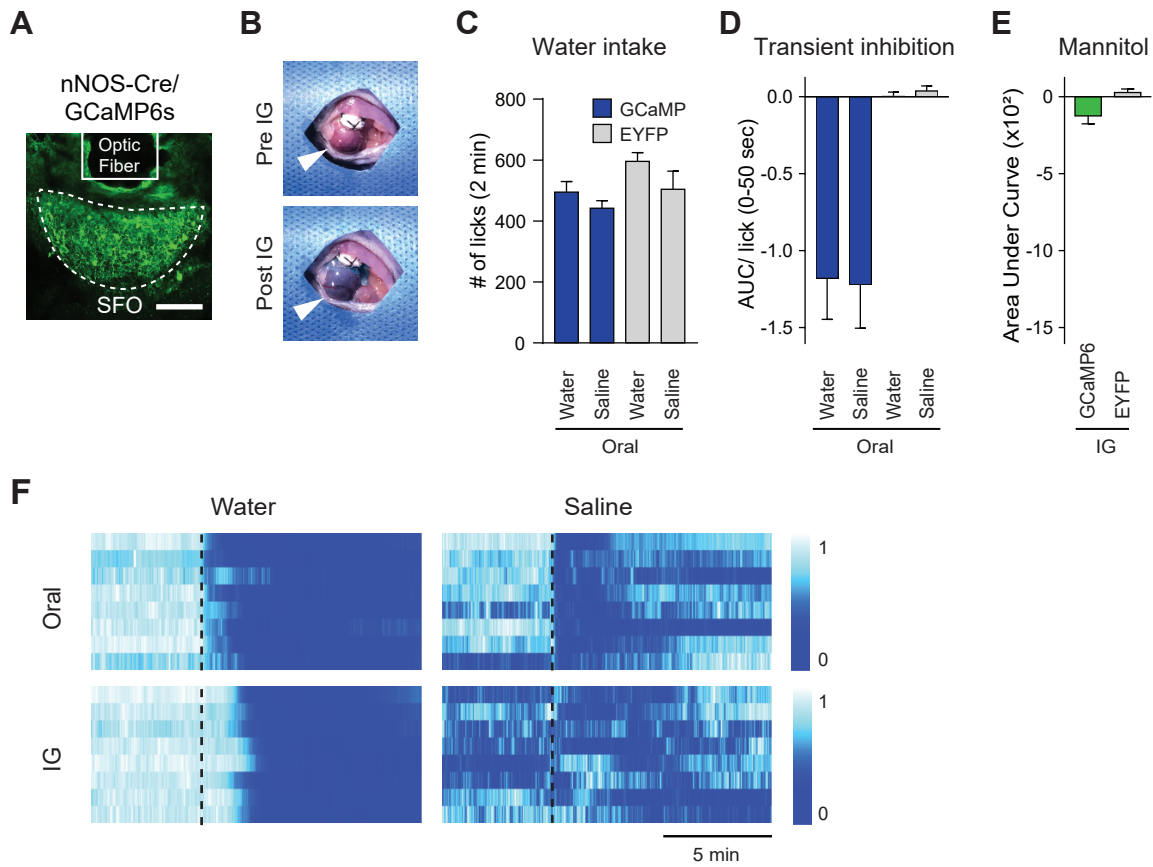


Figure S1. Characterization of SFO^{nNOS} neurons after oral or IG administration of fluid, related to Figure 1. **A**, A representative image of GCaMP6s expression and optic fiber placement in the SFO. **B**, Confirmation of IG surgery. Blue dye was infused into the stomach to ensure successful IG surgery. Before (top) and after (bottom) IG infusion from the same animal are shown. **C**, The number of licks for Figures 1D and 1E. Liquid intake for 2 min was quantified while recording calcium dynamics of SFO^{nNOS} neurons. **D**, Activity change per lick for SFO^{nNOS} neurons ($n = 8$ mice for GCaMP6s, $n = 6$ mice for EYFP). All data were reanalyzed from Figure 1E. **E**, Hypoosmotic stimulus is required for persistent inhibition of SFO^{nNOS} neurons. IG infusion of isotonic mannitol (308 mM) had no effect on the activity of SFO^{nNOS} neurons ($n = 8$ mice for GCaMP6s, $n = 4$ mice for EYFP). **F**, Normalized fluorescence changes of SFO^{nNOS} neurons from individual mice during oral ad lib drinking or IG infusion. Data presented as mean \pm s.e.m. Scale bar, 100 μ m.

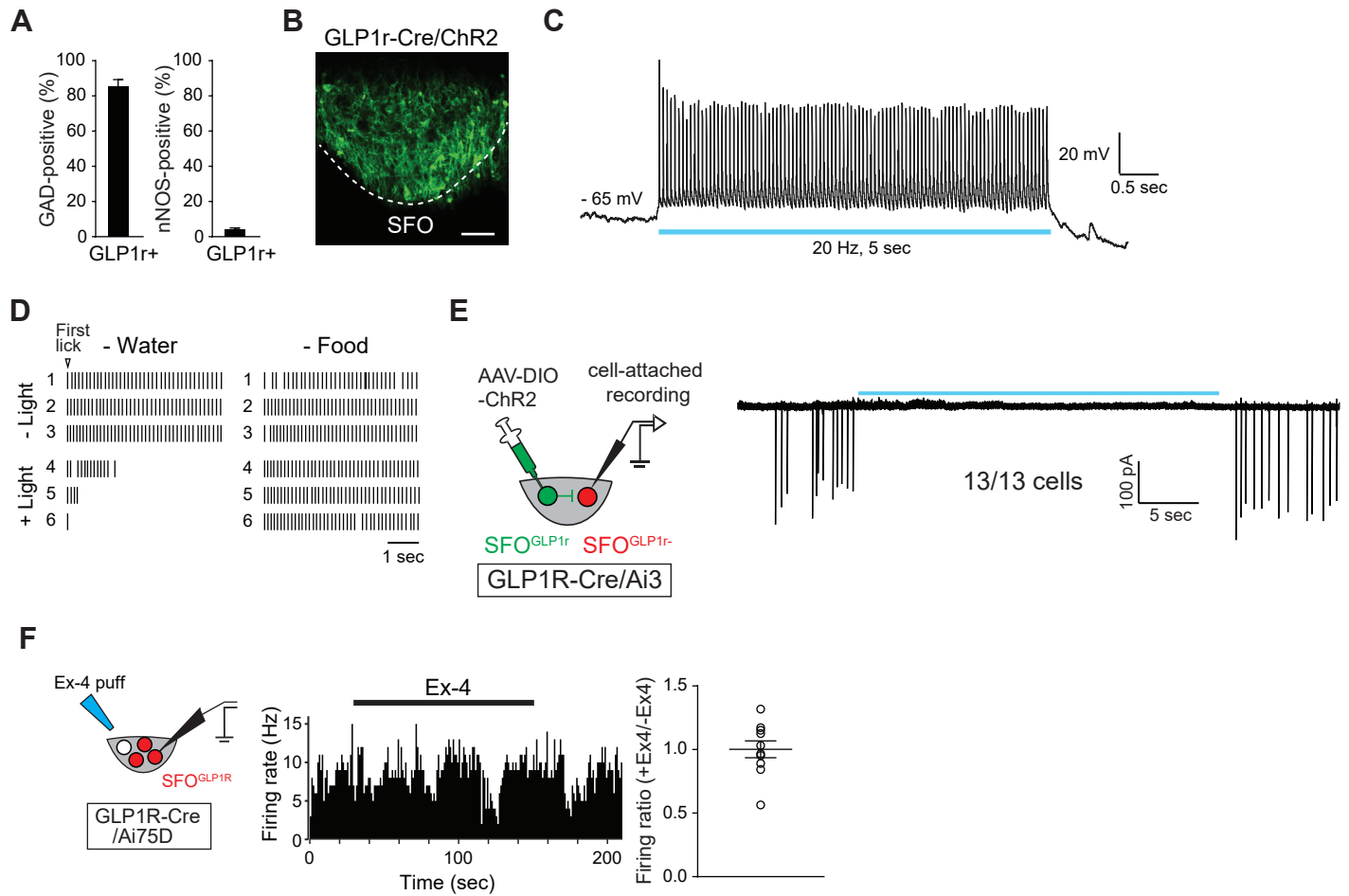


Figure S2. Gain-of-function of SFO^{GLP1r} neurons, related to Figure 2A. **A**, Cell count for Figure 2A. Quantification of the percentage of GAD- or nNOS-positive neurons that coexpressed GLP1r. **B**, A representative image of ChR2-expressing SFO^{GLP1r} neurons (1 out of 5 mice). **C**, Electrophysiological recording in fresh brain slices. Illumination of 475 nm light at 20 Hz activates SFO^{GLP1r} neurons infected with AAV-DIO-ChR2-EYFP (8 out of 8 neurons from 2 mice). **D**, Photostimulation of SFO^{GLP1r} neurons inhibited water intake under water-restricted conditions. However, the same stimulation did not affect Ensure intake under food-restricted conditions. Each black bar indicates a lick event. Representative raster plots from 1 out of 5 mice are shown. **E**, The SFO^{GLP1r} → SFO^{non-GLP1r} monosynaptic connection. Spontaneous firing of all GLP1r-negative neurons tested (13/13 cells) were suppressed by optogenetic activation of SFO^{GLP1r} neurons under cell-attached recording conditions. **F**, Application of an agonist for GLP1r did not induce firing. Electrophysiological recording in SFO^{GLP1r} neurons upon brief application of Exendin-4, a GLP1r-agonist (20 μ M), did not affect the firing rate (10/10 cells). Data presented as mean \pm s.e.m. Scale bar, 50 μ m.

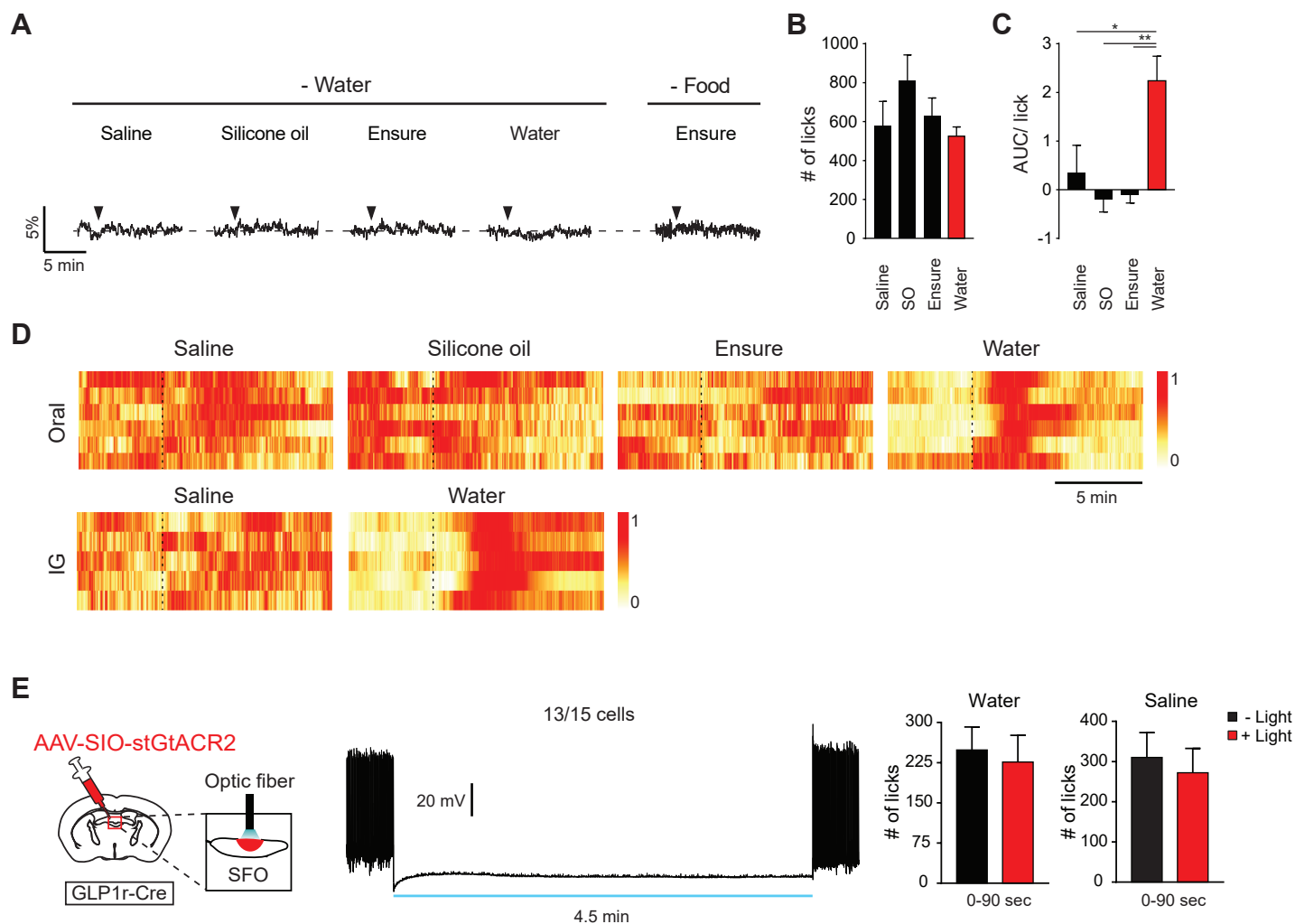


Figure S3. SFO^{GLP1r} neurons are activated by hypoosmotic stimuli in the gut, related to Figure 3. **A**, Control experiments for Figure 3A. Representative responses of SFO^{GLP1r} neurons infected with AAV-DIO-EYFP to different fluids. **B**, The amount of liquid intake for the first 5 min was quantified for Figure 3B. **C**, Fluorescence change per lick for SFO^{GLP1r} neurons (n = 6 mice for GCaMP6s). All data were reanalyzed from Figure 3B. **D**, Normalized fluorescence change of SFO^{GLP1r} neurons from individual mice during oral ad lib drinking or IG infusion. **E**, A diagram for optogenetic inhibition of SFO^{GLP1r} neurons (left). Electrophysiological recording in brain slices. Illumination of 475 nm light inhibits action potential firing in SFO^{GLP1r} neurons infected with AAV-SIO-stGtACR2 (middle, 13 out of 15 neurons). Number of licks before optogenetic inhibition of SFO^{GLP1r} neurons (right, 0-90 sec, Figure 3D). *P<0.05 and **P<0.01 by one-way repeated measures ANOVA (Dunnett's multiple comparisons). Data presented as mean ± s.e.m.

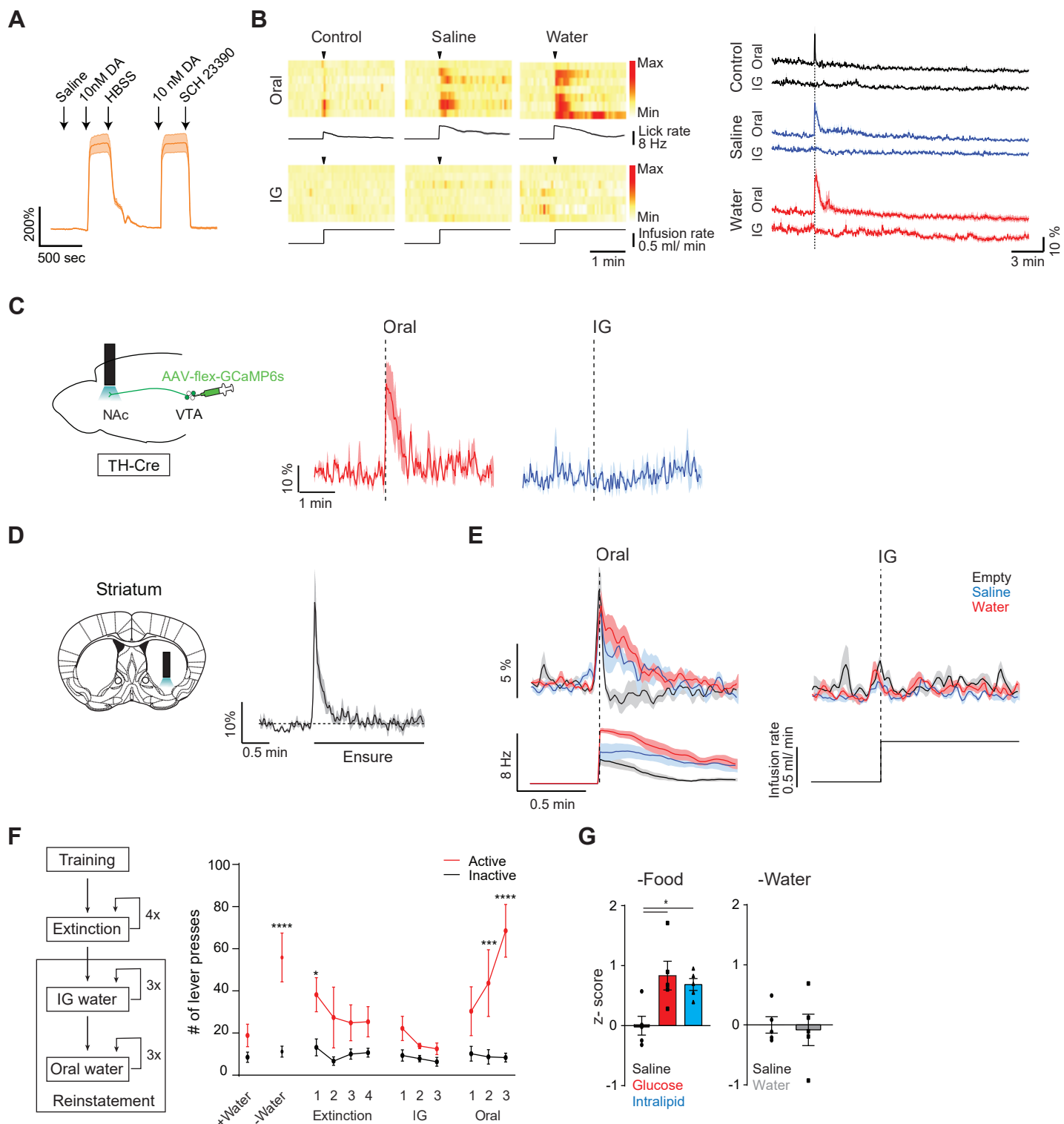


Figure S4. dLight fluorescence change upon fluid administration, related to Figure 4. **A**, dLight is sensitive and photostable in response to low concentration of dopamine during continuous imaging (~30mins, $n = 5$ cells). dLight did not respond to saline but showed increased fluorescence to 10 nM dopamine before the signal was abolished by DRD1 specific antagonist SCH 23390 (right, 5nM). **B**, dLight fluorescence changes from individual mice are shown during oral ad lib intake and IG infusion (left, $n = 7$ mice). For oral access, animals were given an empty bottle (control), isotonic saline, or water. For IG infusion, air, isotonic saline, or water was infused at a speed of 0.5 mL/min for 2 min. Mean traces of dLight fluorescent signals during oral ad-lib drinking or IG infusion (right, $n = 7$ mice). **C**, A diagram of GCaMP6s recording from the projections of VTATH neurons in the NAc. Water was given either orally or via IG infusion. Spontaneous drinking induced robust activation in the NAc when the animal drank water (middle) compared to IG infusion of water (right, $n = 3$ mice). **D**, A diagram of optical recording of dLight fluorescence in the dorsal striatum. DA release is induced by rewarding stimulus (Ensure, $n = 6$ mice). **E**, Peristimulus time histogram of dLight responses to empty, saline, and water. Similar to the NAc, only spontaneous drinking induced DA release in the dorsal striatum ($n = 6$ mice). **F**, A training paradigm for operant conditioning. Mice underwent training and extinction sessions, followed by reinstatement sessions. In reinstatement sessions, animals were first subjected to IG sessions followed by oral sessions. The data for IG and oral reinstatement sessions are from Figure 4H ($n=6$ mice). **G**, Quantified data of dLight responses to intragastric infusion of nutrients or water ($n = 5$ mice). Isotonic saline, 45% glucose or 20% Intralipid was infused into food-deprived mice. Saline or water was infused into water-deprived mice. Post infusion DA release was observed in food-deprived animals (left), but not in water-deprived animals (middle). * $P < 0.05$, *** $P < 0.001$ and **** $P < 0.0001$ by one-way repeated measures ANOVA (Dunnett's multiple comparisons) or two-way repeated measures ANOVA (Bonferroni's multiple comparisons). Data presented as mean \pm s.e.m.